JOURNAL OF GUIDANCE, CONTROL, AND DYNAMICS
Vol. 27, No. 6, November–December 2004

Lambert Guidance Routine Designed to Match Position and Velocity of Ballistic Target

Steven P. Burns* and Jeff J. Scherock†
Johns Hopkins University, Applied Physics Laboratory, Laurel, Maryland 20723-6099

A three-degree-of-freedom interceptor missile simulation designed to rendezvous with a ballistic target is presented. The guidance scheme is designed to match the position and velocity of a ballistic target so that the interceptor will follow the target after the rendezvous. The guidance routine uses Lambert guidance to control the missile during the boost phase and put it on course to meet the ballistic target trajectory. After a long ballistic coast phase, shortly before rendezvous with the ballistic target, a short fourth-stage burn is scheduled to match the velocity of the ballistic target. The two-dimensional Lambert guidance equations are generalized to a three-dimensional coordinate system with the appropriate transformation matrix. The derivation of the equations for the miss distance created by the ΔV maneuver and required modifications to Lambert guidance are presented. Powell's method is used to optimize the missile time of flight to reduce the maneuver ΔV requirements. The missile simulation is used to produce several trajectories and explore the ΔV requirements as a function of downrange and crossrange launch position of the interceptor.

Introduction

THE purpose of this research was to develop a guidance scheme that could be used to put an interceptor missile on the same ballistic path as a ballistic target missile. Also the amount of additional fuel (ΔV) required to perform this trajectory was minimized with Powell's method by varying the interceptor time of flight. Lambert guidance can be used to calculate the needed velocity vector to travel ballistically from position 1 to position 2 in a predetermined time of flight. The Lambert guidance scheme has been used in the past to control a missile in the boost phase to hit a target point on the ground downrange in a desired time.[1,2] In Refs. 1 and 2, Lambert guidance is used during the third stage to give the Strategic Target System target vehicle the velocity vector required to impact the target point downrange. White also mentions a missile launch position offset and a target position offset method to correct for the Lambert guidance assumption of instantaneous rocket motor burn and uniform gravity. This same scheme can be easily extended to put the interceptor missile on a collision course with a ballistic target missile. However, Lambert guidance can only be used to put the missile on a collision course with the target missile, it has no control over the final velocity of the missile when it arrives at the target missile. If the velocity vector of the interceptor missile does not match the velocity vector of the target missile, the two missiles will diverge in position after closest approach. However, if a guidance scheme could be developed such that the interceptor missile had the same velocity vector as the target missile at closest approach, the two missiles would fly on the same ballistic path from that point forward.

The authors extended the classical Lambert guidance routine with the addition of a fourth-stage terminal maneuver to match both the position and the velocity of a ballistic target. Once the position and velocity are matched, the missile will follow the ballistic target for the remainder of the trajectory. In the Appendix, the transformation matrix needed to use the two-dimensional Lambert guidance equations in the three-dimensional Earth-centered inertial (ECI) coordinate system is described. First, a brief description of Lambert guidance is provided. Then the fourth-stage maneuver needed to match target velocity is explained. Next, the derivation of the equations for the miss distance created by the fourth-stage maneuver and required modifications to Lambert guidance are presented. Then the use of Powell's method is described to determine the missile time of flight that minimizes the fourth-stage ΔV requirements. Finally, a few sample trajectories and missile velocity profiles are presented that put the missile on course to match the position and velocity of a ballistic target.

An iterative technique is required to minimize the ΔV between the interceptor missile and ballistic target. An analytic solution could be developed if there was a closed-form solution that expressed the velocity of a ballistic target as a function of time. The burnout velocity and flight-path angle could be set to produce an elliptic orbit that uniquely minimized the interceptor velocity at a particular time in the future when the interceptor arrived at the ballistic target. This analytic equation that predicts velocity at a future time has never been developed, as stated in Refs. 3 and 4. In the words of Bate et al.,[4] "with the Kepler time of flight equations you can easily solve for the time of flight to a future position, however the inverse problem of finding velocity at a future time has never been solved." The universal time of flight equation must be solved with an iterative technique then results plugged into the Kepler constants to calculate the future velocity at time t. There are many references in the literature[3–9] that describe optimal (minimum-fuel) rendezvous trajectories for satellites that are orbiting the Earth. All of these papers are based on the problem of plane change of orbiting satellites. In general, the ΔV maneuvers (and their resulting influence on the trajectory) for plane changes can occur over a time frame of one or more orbit periods (100 min or more). This paper deals with a different but related problem where the vehicles are ballistic missiles (with relatively short flight times) as compared to the orbiting satellite. In the case of a ballistic missile, the ΔV maneuver (and the resulting effect on the trajectory) has to occur over a period of tens to hundreds of seconds to achieve an effective rendezvous with a ballistic target before target impact.

A guidance scheme that can match the position and velocity of a ballistic target can also be useful in the flight-test environment with limited range capability, for example, if the flight-test range had a geography constraint of 4000 km for the maximum distance between target launch and impact, but the target needed a postapogee velocity profile consistent with a ballistic target range of 7000 km. This would allow the higher closing velocity associated with a 7000-km range target, but only require the physical real estate of a 4000-km

Received 25 July 2003; revision received 27 April 2004; accepted for publication 27 April 2004.

*Senior Staff Engineer, Missile Systems Group, 11100 Johns Hopkins Road; steven.burns@jhuapl.edu. Member AIAA.

†Senior Staff Engineer, Missile Systems Group, 11100 Johns Hopkins Road; jeff.scherock@jhuapl.edu. Senior Member AIAA.

range. The effect of missile flight time on trajectory shape will be shown subsequently. The surrogate target could be launched from a downrange position and perform a velocity maneuver at point T_A; from this point on, the surrogate target would have the velocity profile of a 7000-km range missile even though it is flown on a 4000-km flight-test range.

Lambert Guidance

The Lambert problem involves the propagation of a body in a Newtonian central gravity field. The solution provides the instantaneous velocity required to travel from an initial position $\boldsymbol{r}_1$ to a final position $\boldsymbol{r}_2$ in a specified time under the influence of only gravity. In the scenario of a boosting missile in the atmosphere (propulsive and atmospheric forces as well as gravity present), the Lambert problem is solved at each integration time step. The current missile velocity $\boldsymbol{V}_M$ is subtracted from the required Lambert velocity $\boldsymbol{V}_{\text{LAMBERT}}$ to compute the velocity to be gained, $\boldsymbol{V}_G$ as shown in Fig. 1. The missile is commanded to accelerate in the direction of $\boldsymbol{V}_G$; in the lower atmosphere, a fixed flyout flight-path angle schedule is followed to curtail the atmospheric drag losses. Missile thrusting is terminated when $\boldsymbol{V}_G$ reaches a threshold tolerance level, and the missile flies ballistically to the intended target.

The missile simulation to accomplish the study was adapted from several two-dimensional in-plane strategic engagement Lambert guidance FORTRAN routines.[10] The basic framework of the simulation was maintained, but expanded to permit three-dimensional engagements with realistic atmospheric effects. The simulation is a three-degree-of-freedom (3-DOF) model using a second-order Runge–Kutta integration scheme. The Earth is modeled as a nonrotating sphere, providing an adequate level of fidelity for preliminary analysis.

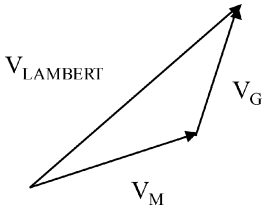

Fig. 1 Velocity diagram for Lambert guidance.

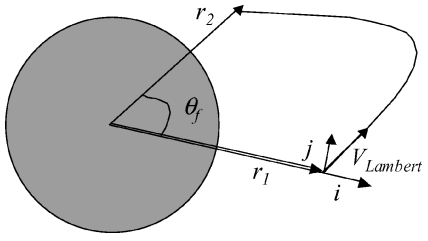

Fig. 2 Lambert plane containing the initial and desired position vectors.

The formulation of the computational frame for the three-dimensional Lambert guidance scheme was adapted from Ref. 11. The derivation will be briefly summarized.

Figure 2 shows the plane containing the initial $\boldsymbol{r}_1$ and final $\boldsymbol{r}_2$ position vectors, which is defined as the Lambert computational frame. For our study $\boldsymbol{r}_1$ is the instantaneous position of the interceptor missile and $\boldsymbol{r}_2$ is the intended rendezvous point with the ballistic target. The angle subtended by the flight, θ_f, can be formulated as

$$\theta_f = \cos^{-1}(\boldsymbol{r}_1 \cdot \boldsymbol{r}_2/|\boldsymbol{r}_1\|\boldsymbol{r}_2|) \tag{1}$$

All of the trajectories used for this study had ranges significantly less than halfway around the Earth ($\theta_f < 180$ deg). However, for angles greater than 180 deg, $\theta_f = 360 \text{ deg} - \theta_f$. Whereas no closed-form solution of the velocity as a function of time exists, the velocity can be found through iteration. The flight-path angle γ is selected, and V and time of flight t_f are computed as shown in Fig. 3.

It is convenient to define $\lambda = |\boldsymbol{r}_1|V^2/\mu$, a dimensionless constant that is the ratio of twice the kinetic energy to potential energy. This quantity plays a central role in determining the nature of the trajectory. If $0 < \lambda < 2$, the trajectory is elliptical; if $\lambda > 2$, it is hyperbolic; and if $\lambda = 2$, it is a parabolic trajectory. The range of possible values of λ is limited, as suggested in Refs. 10 and 11, to include only elliptical trajectories. The secant iteration method is used to converge on the solution to Lambert's problem efficiently.

To convert the Lambert solution shown in Figs. 2 and 3 from the two-dimensional plane containing the trajectory to the three-dimensional ECI computational frame of the simulation, the transformation matrix described in the Appendix was used. The $\boldsymbol{V}_{\text{LAMBERT}}$ velocity vector is the Lambert velocity vector in ECI coordinates. The missile is commanded to thrust along the $\boldsymbol{V}_G$ axis to align $\boldsymbol{V}_M$ with $\boldsymbol{V}_{\text{LAMBERT}}$. The simulated engagement begins after the target has burned out at an altitude above the sensible atmosphere. The target position, anytime before reentry, can be propagated in a gravity field using its state vector information at burnout. Inside the simulation, the state vector at burnout is known based on the input target trajectory. The interceptor is commanded to fly toward the calculated position of the target at the rendezvous time. In this way an intercept can be simulated at several stations along the target trajectory using the same guidance routine. This permitted the study of several schemes and missile interceptor configurations to obtain optimal performance.

For a real-world missile flight, the target's state vector would have to be computed in real time based on external radar sensor observations of the ballistic missile. The target state vector produced by a radar would also have a covariance associated with it. This covariance would describe how the error in the state vector grows with time. The final stage of the interceptor would also have to account for extra divert fuel required to handle the error volume defined by the covariance.

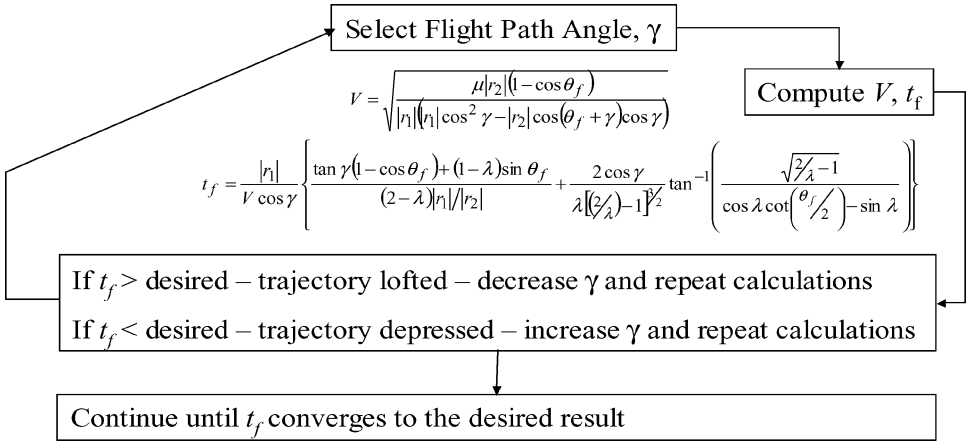

Fig. 3 Lambert solution process.

Fourth-Stage Maneuver to Match Target Velocity

The missile simulation uses Lambert guidance to arrive at the same point in three-dimensional space as the ballistic target. However, Lambert guidance does not have direct control of the velocity of the missile when it arrives at the target point. If the velocity vector is not changed, the missile will not follow the same ballistic path of the target after arrival at the target. A short fourth-stage burn was devised to change the missile's velocity vector to match the target. Figure 4 shows the entire guidance scheme from Lambert guidance used during the boost phase to a fourth-stage maneuver just before rendezvous. Figure 4 shows the missile velocity $\boldsymbol{V}_M$, target velocity $\boldsymbol{V}_T$, $\Delta\boldsymbol{V}$, and the thrust vector $\boldsymbol{T}$ (directed along the $\Delta\boldsymbol{V}$ vector) designed to change the missile velocity vector during the fourth-stage maneuver. The x, y, and z components of the thrust vector are directed along the $\Delta\boldsymbol{V}$ vector:

$$T_X = (\Delta\boldsymbol{V}_X/\Delta\boldsymbol{V})T, \quad T_Y = (\Delta\boldsymbol{V}_Y/\Delta\boldsymbol{V})T, \quad T_Z = (\Delta V_Z/\Delta\boldsymbol{V})T$$
$$\text{where} \qquad T = I_{\text{sp}}\dot{W} \tag{2}$$

The thrust magnitude is simply the specific impulse I_{sp} times the propellant burn rate $\dot{W}$. Drag forces can be ignored because the fourth-stage maneuver takes place in the exoatmosphere. The fourth-stage vehicle starts out with an initial weight of $W_{4\text{th}}$ and loses weight as the rocket motor burns. The equation of motion for the fourth-stage vehicle along the $\Delta\boldsymbol{V}$ vector is

$$f = ma, \qquad T = (W/g)a, \qquad gI_{\text{sp}}\dot{W} = (W_{4\text{th}} - \dot{W}t)a \tag{3}$$

The acceleration due to gravity can be ignored because both the missile and the ballistic target are in the same gravity field. Also the force due to gravity is small compared to the force produced by the rocket motor thrust. The equation will be used to calculate a burn time needed to reduce the $\Delta\boldsymbol{V}$ between the missile and ballistic target; this is a relative velocity, not an absolute velocity. This equation can be solved for the fourth-stage acceleration due to the simple fourth-stage motor burn as

$$a = gI_{\text{sp}}[\dot{W}/(W_{4\text{th}} - \dot{W}_t)] \tag{4}$$

The acceleration can be integrated with respect to time to determine the velocity as

$$V = \int a\,\mathrm{d}t = gI_{\text{sp}}\int \frac{\dot{W}}{W_{4\text{th}} - \dot{W}_t}\,\mathrm{d}t$$
$$V = gI_{\text{sp}}\left[\ell_n\left(\frac{W_{4\text{th}}}{W_{4\text{th}} - \dot{W}t}\right)\right] \tag{5}$$

Equation (5) is a form of the standard rocket equation. The following equation shows the velocity equation solved for the burn time ΔT needed to achieve a velocity change of $\Delta\boldsymbol{V}$,

$$\Delta T = (W_{4\text{th}}/\dot{W})[1 - \exp(-\Delta\boldsymbol{V}/gI_{\text{sp}})] \tag{6}$$

so that the missile simulation will execute a fourth-stage burn in the direction of the $\Delta\boldsymbol{V}$ vector when it is ΔT seconds away from the target rendezvous point. However, the consequence of this short fourth-stage burn is the missile will not achieve the desired target position. This is because the fourth-stage burn has pushed the missile away from the ballistic target point. To compensate for this, the Lambert guidance routine will guide the missile during boost to a new point $\boldsymbol{R}_{\text{offset}}$. Figure 5 is a closeup from Fig. 4, which shows the relationship of $\boldsymbol{R}_{\text{offset}}$, $\boldsymbol{R}_T$ (the intended ballistic target point), and $\Delta\boldsymbol{R}$ (the miss distance due to the fourth-stage burn),

$$\boldsymbol{R}_{\text{offset}} = \boldsymbol{R}_T - \Delta\boldsymbol{R}$$

The authors derived the equation to calculate the amount of position offset $\Delta\boldsymbol{R}$ required to adjust for the fourth-stage burn. Equation (5)

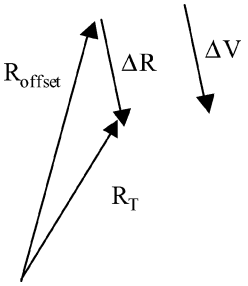

Fig. 5 Position offset due to fourth-stage burn.

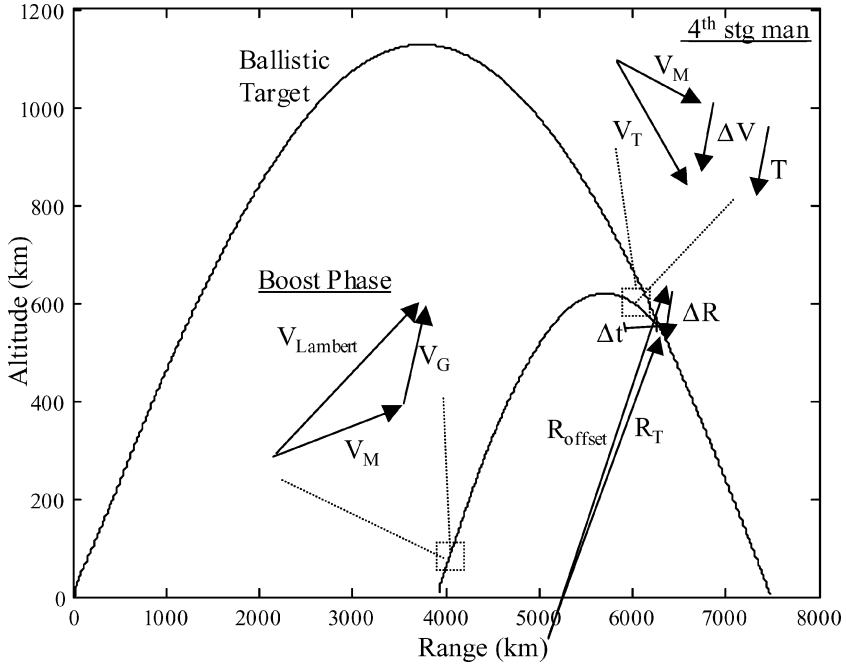

Fig. 4 Guidance scheme designed to match position and velocity of ballistic target.

(velocity equation) can be integrated a second time to derive the distance the fourth-stage travels due to the fourth-stage burn. The following equation shows the distance traveled by the fourth-stage as a function of the fourth-stage burn time:

$$\boldsymbol{R} = \int V\,\mathrm{d}t = gI_{\mathrm{sp}} \int \ell_n\left(\frac{W_{4\mathrm{th}}}{W_{4\mathrm{th}} - \dot{W}t}\right)\mathrm{d}t$$

$$\Delta\boldsymbol{R} = gI_{\mathrm{sp}}\left[\left(\frac{W_{4\mathrm{th}}}{\dot{W}} - \Delta t\right)\ell_n\left(\frac{W_{4\mathrm{th}} - \dot{W}\Delta t}{W_{4\mathrm{th}}}\right) + \Delta t\right] \quad (7)$$

The x, y, and z components of the $\Delta\boldsymbol{R}$ vector are directed along the $\Delta\boldsymbol{V}$ vector as shown in the following equation and Fig. 5:

$$\boldsymbol{R}_X = (\Delta\boldsymbol{V}_X/\Delta\boldsymbol{V})\Delta R, \qquad \boldsymbol{R}_Y = (\Delta\boldsymbol{V}_Y/\Delta\boldsymbol{V})\Delta R$$

$$\boldsymbol{R}_Z = (\Delta\boldsymbol{V}_Z/\Delta\boldsymbol{V})\Delta R \quad (8)$$

To summarize, the final simulation run uses Lambert guidance during boost to guide to a point offset from the ballistic target point by $\Delta\boldsymbol{R}$. When the time to intercept reaches ΔT, the short fourth-stage burn is executed and the missile flies through the ballistic target point with the required velocity to follow the same ballistic path as the target.

Minimize ΔV with Interceptor Time of Flight

The interceptor missile is launched at some downrange position compared to the ballistic target. The shape of the trajectory that the missile flies toward the target is determined by two parameters: the time the missile arrives at the ballistic target, T_A, and the time the missile launches, T_D; Both of these times are relative to the ballistic target burnout. Figure 6 shows two different trajectories that Lambert guidance will fly based on the amount of time available to get to the ballistic target point.

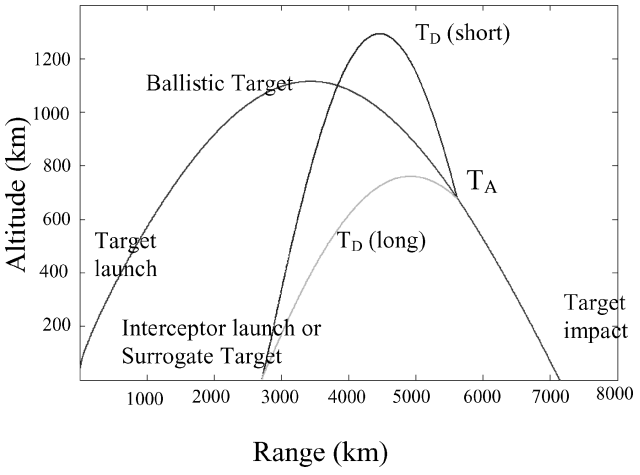

Fig. 6 Effect of missile flight time on trajectory shape.

With a long time available (short launch delay time), Lambert guidance flies a high loft trajectory and intersects the ballistic target trajectory at a steep angle. With a shorter time available (long launch delay time), Lambert guidance flies a low loft trajectory and intersects the ballistic target trajectory at a more favorable angle. The angle the missile trajectory intersects the ballistic target trajectory directly relates to the magnitude of the $\Delta\boldsymbol{V}$ vector needed to change the missile velocity to match the ballistic target velocity. In this case the low loft trajectory results in a smaller ΔV. A small ΔV is desired because this will reduce the fourth-stage propellant required to execute the fourth-stage burn and match the ballistic target velocity. By minimizing the fourth-stage propellant weight, you can decrease the overall weight of the total missile.

There is an optimal combination of ballistic target arrival time and missile launch delay time that minimizes the ΔV difference between the missile and ballistic target. Figure 7 shows the ΔV difference as a function of ballistic target arrival time and missile launch delay time. This was produced with 10,164 different simulation runs, 84 different arrival times (1000–1400 s), and 121 different launch delay times (100–500 s).

This is appeared to be a simple problem of minimization of ΔV with two inputs. Powell's method (see Ref. 12) in multidimensions was used to converge to the combination of T_A and T_D that produce the smallest ΔV. Powell's method is a successive line minimization algorithm. Figure 7 shows the path that Powell's method traverses from the first guess to the optimal point. The individual black points are the specific points that Powell's method calculates. The routine starts at $T_D = 100$ s, $T_A = 950$ s, and high ΔV. First the Powell method takes small steps along the T_A axis, and then it takes increasingly larger steps until a user-imposed limit is reached. Then the Powell method traverses the T_D axis until the minimum ΔV point is reached. The Powell method required 41 iterations to reach the minimum ΔV point. This is a significant improvement over the brute force method (10,164 simulation runs) used to characterize the three-dimensional surface plot of ΔV vs T_A and T_D. Several simulation runs showed this is not a two-dimensional problem, just a one-dimensional optimization problem. The Powell optimization always went to the largest user-specified target arrival time T_A and then used T_D for the true optimization. Missile launch delay time T_D is the only parameter that is needed in the ΔV optimization scheme. This makes sense from a dimensional analysis point of view. Although two different time values T_A and T_D were used in

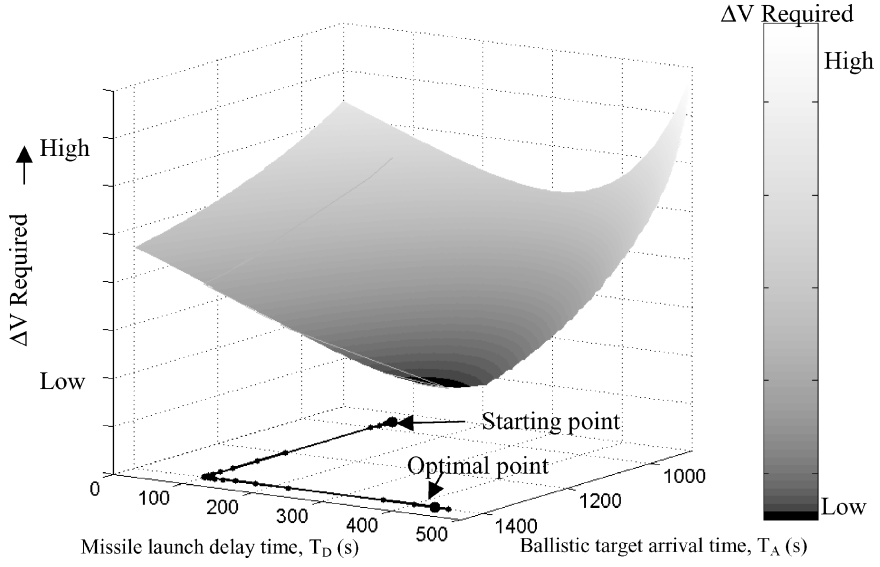

Fig. 7 Effect of missile launch delay and ballistic target arrival time on ΔV required.

the Powell optimization scheme, the Lambert trajectory only has a single time value, T_f for time of flight.

The preceding example minimized the ΔV for one specific missile launch point. The next step was to see how the optimum interceptor launch delay changed at various downrange and crossrange launch positions. The simulation was set up to vary the downrange and crossrange launch position of the interceptor relative to the ballistic target trajectory and then have the Powell method compute the optimal time of flight T_f for each particular launch point. All of the interceptor simulations rendezvous with the same point on the ballistic target at $T_A = 1400$ s. Figure 8 shows the optimal missile launch delay T_D as a function of interceptor launch position. A launch delay $T_D = 1000$ s corresponds to a time of flight $T_f = 400$ s, and a launch delay $T_D = 200$ s corresponds to a time of flight $T_f = 1200$ s. Figure 8 shows that the optimal launch delay time is a short interceptor launch delay for interceptor launch positions close to the target launch position and a long interceptor launch delay for interceptor launch positions far downrange from the target launch position. This means that it actually pays to delay your interceptor launch if your interceptor launch point is far downrange from the target launch point. Figure 8 also shows the effect of crossrange offset on the optimal launch delay. The optimal interceptor launch delay decreases as the interceptor launch point moves crossrange off the ballistic trajectory.

Iterate to Eliminate Miss Distance Due to Integrated Gravity Effect

The first run of the simulation propagates the missile to the target position $\boldsymbol{R}_T$ using Lambert guidance. Then the ΔV between the missile and target is computed at the point of closest approach. This is followed by computing the $\Delta \boldsymbol{R}$ offset needed to adjust for the fourth-stage burn to correct for the ΔV difference. The second simulation run now guides to $\boldsymbol{R}_{\text{offset}}$ and executes the fourth-stage burn to arrive at the same position and velocity at the target. However, the velocity of the missile does not match the velocity of the target exactly. This is because the missile takes a slightly different path in the second run guiding to $\boldsymbol{R}_{\text{offset}}$ then it did in the first run guiding to $\boldsymbol{R}_T$. This change in position results in a small error in final velocity caused by the integrated effect of gravity differences caused by the small differences in missile position throughout flight. The gravity-gradient effect is small for short burn times, that is, fourth-stage burn, but the gravity-gradient effect is not small over long prediction intervals from burnout to intercept; these differences require an iteration of the aimpoint strategy. To remedy this, the ΔV calculation is refined with subsequent simulation runs until convergence is obtained. The process is as follows: Calculate ΔV, rerun guiding to $\boldsymbol{R}_{\text{offset}}$ and repeat until ΔV does not change with successive iterations. The ΔV converges quickly, generally after only two or three iterations. Figure 9 shows the distance between the target and missile around the arrival time T_A. The first run shows the missile achieving the target position at time T_A, but then rapidly moving away because of the large velocity difference between the target and missile. The first iteration with a fourth-stage ΔV maneuver shows the missile achieving the target position at time T_A, but then slowly moving away because of a small velocity difference due to the integrated effect of gravity. The second iteration on ΔV shows the missile achieving the target position at time T_A and the target velocity; with these matched conditions, the missile follows the target for the remainder of the ballistic flight.

This entire guidance process used to match the position and velocity of a ballistic target with the minimum amount of fourth-stage fuel is summarized in the flowchart shown in Fig. 10 with use of Eqs. (6) and (7).

Final Results

The missile 3-DOF simulation was used to produce several missile trajectory and velocity profiles that matched the position and velocity of a ballistic target at a specified arrival time. Figure 11 shows the downrange-altitude trajectory for three different missile flyouts and the ballistic target trajectory they are trying to match. All three trajectories are intended to arrive at the ballistic target at time T_A. Trajectory A follows a simple Lambert guidance to arrive at the

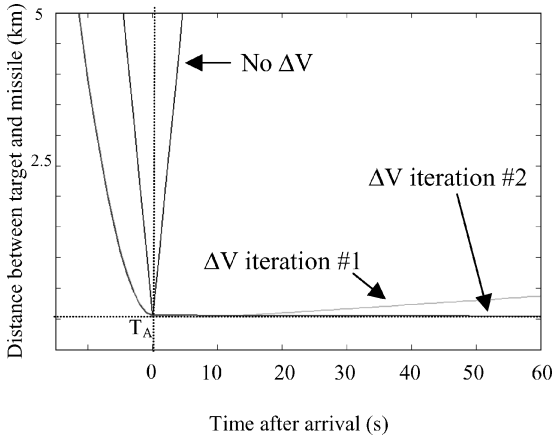

Fig. 9 Distance between target and missile for successive ΔV iterations.

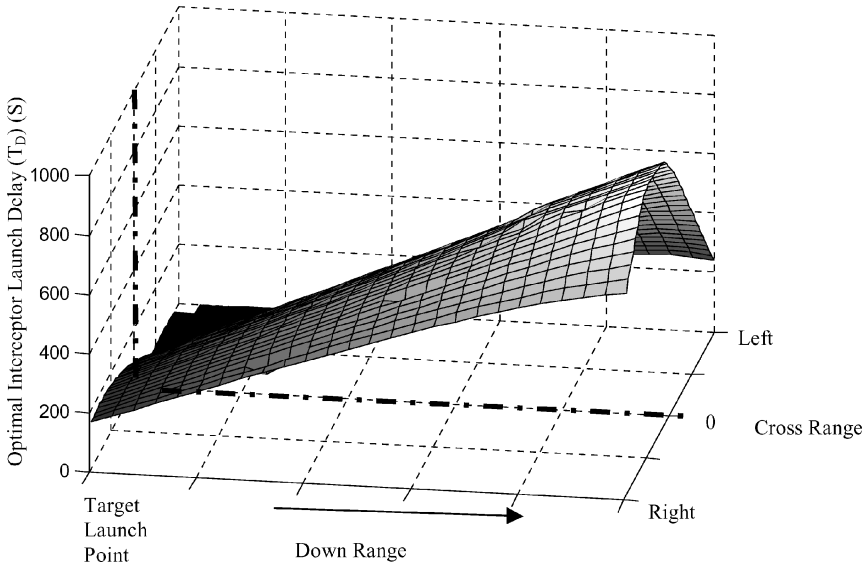

Fig. 8 Optimal interceptor launch delay to minimize ΔV as a function of interceptor launch point.

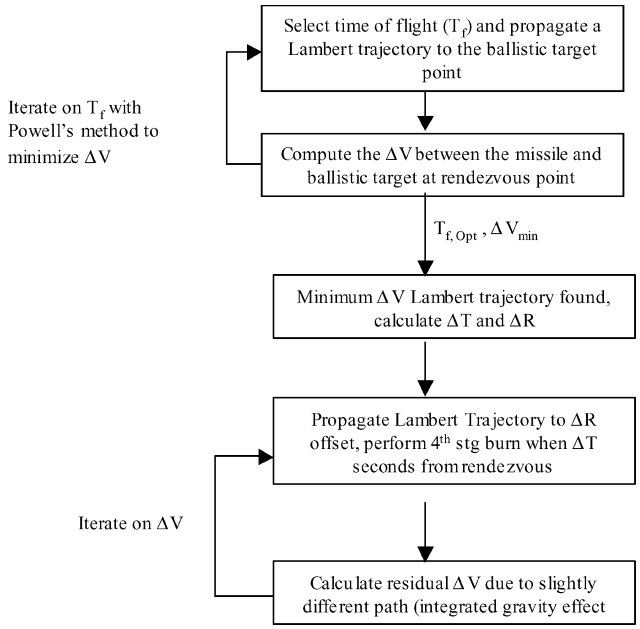

Fig. 10 Guidance process used to match the position and velocity of a ballistic target.

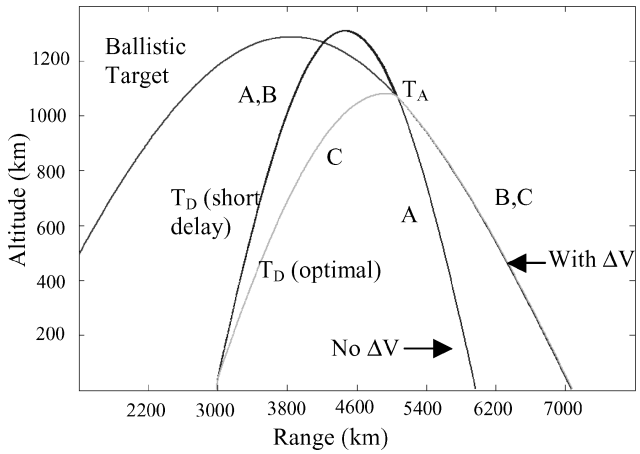

Fig. 11 Interceptor trajectory that matches the position and velocity of a ballistic target.

target position but has no fourth-stage maneuver to match the target velocity. Trajectory A quickly departs the ballistic target trajectory after the arrival time. Trajectory B follows Lambert guidance to arrive at the target and has a fourth-stage maneuver to match target velocity. Trajectory B has a short delay time and follows a high loft to arrive at the ballistic trajectory at a steep angle. As a result, the fourth-stage ΔV requirement is large. Trajectory C launches at the optimal (optimized with Powell's method) delay time and follows a lower loft trajectory to arrive at the ballistic target trajectory at a much more favorable angle. As a result, the ΔV requirement is much smaller than trajectory B. This ΔV difference can be seen in Fig. 12, which shows the velocity profiles of the three trajectories. Because trajectory C approaches the ballistic target trajectory at a favorable angle, its fourth-stage ΔV requirement is reduced by about 40% when compared to trajectory B. The ΔV requirement is also reduced due to the lower loft trajectory. Trajectory B loses more velocity due to the greater change in potential energy because of the higher loft. Thus, when it comes time to match the ballistic target velocity, trajectory B has to make up more of a velocity deficit.

The results shown in Fig. 11 led to the following question: Does the optimal encounter always happen when the missile flyout approaches the ballistic target at the apogee point of the interceptor missile? From an absolute velocity magnitude, this would make sense because the interceptor missile velocity is minimum at apogee;

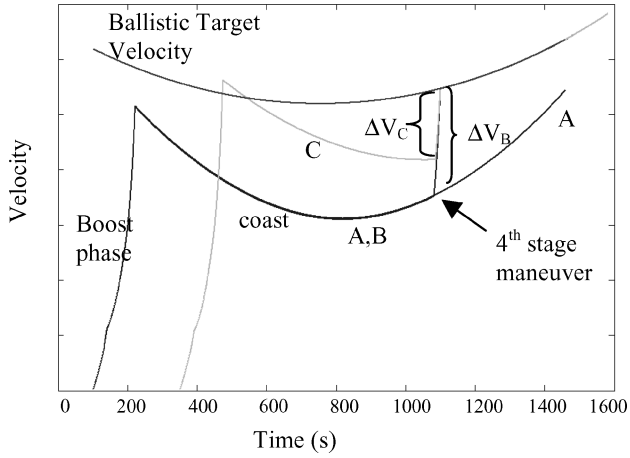

Fig. 12 Interceptor velocity needed to match position and velocity of a ballistic target.

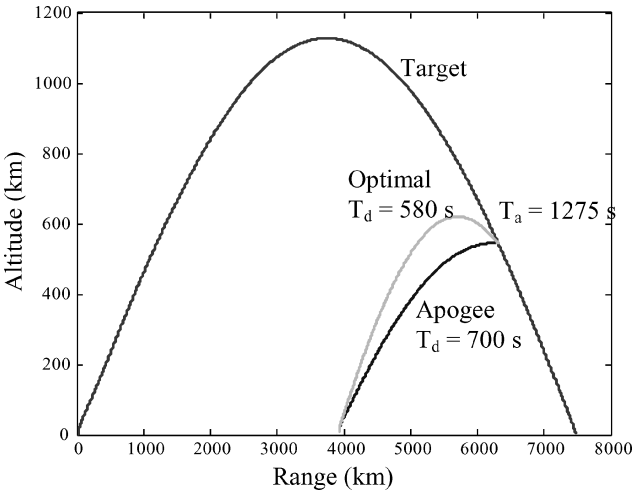

Fig. 13 Comparison of optimal trajectory to apogee trajectory.

therefore, the ΔV required to match the target velocity should be smallest. To test out this notion, a second intercept case was run. This time the intercepting missile was launched much farther downrange and the intended arrival point to the ballistic target was also moved farther downrange. Figure 13 shows the trajectory results of this engagement simulation. The trajectory labeled apogee results from the intercepting missile arriving at the ballistic target at its own apogee point (minimum velocity). Then Powell's method with Lambert guidance and fourth-stage velocity maneuver was used to minimize the ΔV required to match the ballistic target position after the arrival. The trajectory shown as optimal is Powell's method minimum ΔV trajectory. This case proves that it is not always optimal to arrive at the ballistic target at the apogee point on the intercepting missile. In general, Battin[3] points out that the Hohmann transfer with a doubly cotangent orbit is only optimal when the transfer angle $\theta f = 180$ deg. For all cases in this study, the transfer angle was significantly less than 180 deg. Figure 14 shows a closeup of Fig. 13. The optimal trajectory follows a higher loft and arrives at the ballistic target with a more favorable angle. The velocity vectors at target arrival are also shown in Fig. 14. The velocity vector diagram (drawn to scale) shows that the interceptor velocity vector for the optimal case is much closer to the target velocity vector than for the case when the interceptor arrives at apogee. This results in a ΔV requirement that is 20% smaller for the optimal case than for the apogee case. This particular case shows that there is, indeed, a need to use Powell's method to search for the optimal launch delay.

The second point to notice is that the optimal trajectory also used less propellant during the boost phase. The magnitude of the velocity vector at booster burnout and total boost phase burntime

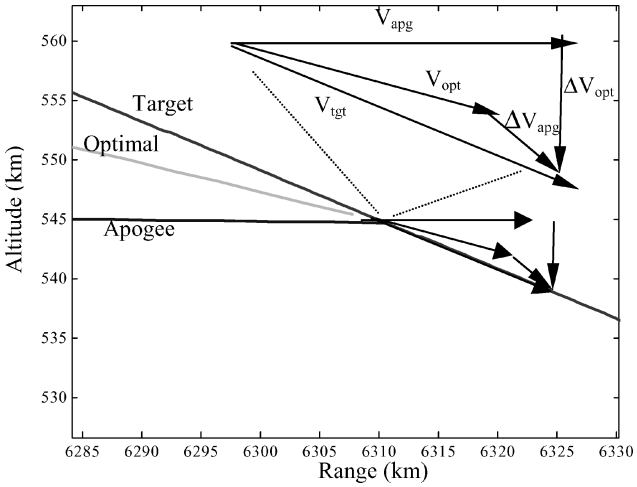

Fig. 14 Velocity diagram for an optimal trajectory and apogee trajectory.

was smaller for the optimal trajectory. This can also be seen by the smaller magnitude of the optimal trajectory velocity vector in Fig. 14. This point is relevant to a point made in the Introduction that this guidance scheme could be used to fly a surrogate target with a 7000-km velocity profile in a physical range of 4000 km.

Conclusions

A modified Lambert guidance routine has been developed that matches both the position and velocity of a ballistic target. The traditional Lambert guidance scheme was used to match the position of the target. The authors developed a modification to Lambert guidance to also match the velocity of a ballistic target. The velocity was matched with the addition of a fourth-stage maneuver. The interceptor time of flight can be optimized to minimize the fourth-stage ΔV requirement. The burn rate $\dot{W}$ of the fourth-stage maneuver can be limited to satisfy a maximum acceleration load on the fourth-stage. A 3-DOF simulation was developed and run to show the trajectory and velocity profiles of a typical missile flyout that puts the fourth-stage vehicle on course to follow the ballistic target. The final guidance routine proved to be a very efficient method to match both position and velocity of a ballistic target. The iterative guidance scheme runs fast enough that it could be implemented in real time for a real-world ballistic target.

The new guidance scheme showed that it is possible for an interceptor missile to be put on the same ballistic path as a target missile. The simulation showed that the fourth-stage ΔV requirements increase the farther crossrange and downrange the interceptor launch point is compared to the target ballistic path. Also the optimal interceptor missile launch delay increases as the interceptor launch point moves downrange compared to the target launch point. In other words, as the interceptor launch point moves downrange, it actually helps to delay the launch of the interceptor to a later time. The results of the simulation showed that the Powell method can be used to find the interceptor time of flight that minimizes the fourth-stage ΔV requirement.

Appendix: Computation of Transformation Matrix from Two-Dimensional Lambert Plane to Three-Dimensional ECI Plane

To convert the Lambert solution from the two-dimensional plane containing the trajectory ($\boldsymbol{r}_1$ and $\boldsymbol{r}_2$ vector) to the three-dimensional ECI computational frame of the simulation, the following transformation is used. The ECI (XYZ) to Lambert computational frame (IJK) is defined using three successive rotations shown in Fig. A1. The first is a rotation about Z by the longitude (lon) of the missile position. Next, rotate about the new Y (Y') by the angle of latitude (lat). Multiplication of the preceding intermediate transformation yields the following matrix:

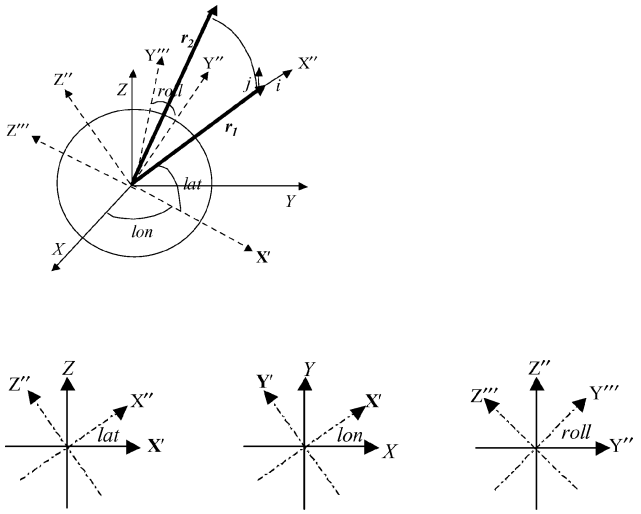

Fig. A1 Transformation from two-dimensional Lambert plane to three-dimensional ECI plane.

$$\begin{bmatrix} \cos(\text{lat}) & 0 & -\sin(\text{lat}) \\ 0 & 1 & 0 \\ \sin(\text{lat}) & 0 & \cos(\text{lat}) \end{bmatrix} \begin{bmatrix} \cos(\text{lon}) & \sin(\text{lon}) & 0 \\ -\sin(\text{lon}) & \cos(\text{lon}) & 0 \\ 0 & 0 & 1 \end{bmatrix}$$

$$= \begin{bmatrix} \cos(\text{lat})\cos(\text{lon}) & \cos(\text{lat})\sin(\text{lon}) & -\sin(\text{lat}) \\ -\sin(\text{lon}) & \cos(\text{lon}) & 0 \\ -\sin(\text{lat})\cos(\text{lon}) & -\sin(\text{lat})\sin(\text{lon}) & \cos(\text{lat}) \end{bmatrix} \quad \text{(A1)}$$

The second row of matrix (A1) represents the pointing vector of $\boldsymbol{Y}''$ in the ECI frame. The arccosine of the dot product of the $\boldsymbol{j}$ unit vector and $\boldsymbol{Y}''$ unit pointing vector represents the roll angle about X'' necessary to align the (X''', Y''', Z''') frame with the Lambert computational frame. The $\boldsymbol{j}$ unit vector and the $\boldsymbol{Y}''$ unit vector are defined as

$$\boldsymbol{r}_P = \boldsymbol{r}_1 \times \boldsymbol{r}_2, \qquad \boldsymbol{r}_{CR} = \boldsymbol{r}_P \times \boldsymbol{r}_1, \qquad \boldsymbol{j}_{UV} = \boldsymbol{r}_{CR}/\|\boldsymbol{r}_{CR}\|$$

$$\boldsymbol{Y}'' = -\sin(\text{lon})\boldsymbol{X} + \cos(\text{lon})\boldsymbol{Y}, \qquad \text{roll} = \cos^{-1}(\boldsymbol{Y}'' \cdot \boldsymbol{j}_{UV})$$

The roll angle must be checked to ensure $\boldsymbol{Y}'''$ is aligned with $\boldsymbol{j}$ and not $-\boldsymbol{j}$. If it is aligned with $-\boldsymbol{j}$, the roll angle is defined as $2\pi - \text{roll}$. Then the final transformation matrix from ECI to IJK is

$$T_{\text{ECI}}^{IJK} = \begin{bmatrix} \cos(\text{lat})\cos(\text{lon}) & \cos(\text{lat})\sin(\text{lon}) & -\sin(\text{lat}) \\ -\cos(\text{roll})\sin(\text{lon}) + \sin(\text{roll})\sin(\text{lat})\cos(\text{lon}) & \cos(\text{roll})\cos(\text{lon}) + \sin(\text{roll})\sin(\text{lat})\sin(\text{lon}) & \sin(\text{roll})\cos(\text{lat}) \\ \sin(\text{roll})\sin(\text{lon}) + \cos(\text{roll})\sin(\text{lat})\cos(\text{lon}) & -\sin(\text{roll})\cos(\text{lon}) + \cos(\text{roll})\sin(\text{lat})\sin(\text{lon}) & \cos(\text{roll})\cos(\text{lat}) \end{bmatrix} \quad \text{(A2)}$$

The transformation matrix from IJK to ECI, T_{IJK}^{ECI}, is the transpose of the preceding matrix. The T_{IJK}^{ECI} matrix can be used to transform the two-dimensional Lambert velocity into three-dimensional ECI velocity. The velocity in the ECI frame is calculated as follows:

$$\boldsymbol{V}_{\text{Lambert}} = \begin{bmatrix} \boldsymbol{V}_X \\ \boldsymbol{V}_Y \\ \boldsymbol{V}_Z \end{bmatrix} = T_{IJK}^{\text{ECI}} \begin{bmatrix} \boldsymbol{V}_I \\ \boldsymbol{V}_J \\ 0 \end{bmatrix} \quad \text{(A3)}$$

References

[1]White, J. E., "A Lambert Targeting Procedure for Rocket Systems That Lack Velocity Control," *Proceedings of the Guidance, Navigation, and Control Conference*, AIAA, Washington, DC, 1989, pp. 146–154.

[2]White, J. E., "Guidance and Targeting for the Strategic Target System," *Journal of Guidance, Control, and Dynamics*, Vol. 15, No. 6, 1992, pp. 1313–1319.

[3]Battin, R., *An Introduction to the Mathematics and Methods of Astrodynamics*, AIAA, Washington, DC, 1987, pp. 526–528.

[4]Bate, R., Mueller, D., and White, J., *Fundamentals of Astrodynamics*, Dover, New York, 1971, pp. 193–199.

[5]Prussing, J. E., "A Class of Optimal Two-Impulse Rendezvous Using Multiple-Revolution Lambert Solutions," *Journal of the Astronautical Sciences*, Vol. 48, No. 2–3, 2000, pp. 131–148.

[6]Humi, M., "Fuel-Optimal Rendezvous in a General Central Force Field," *Journal of Guidance, Control, and Dynamics*, Vol. 16, No. 1, 1993, pp. 215–217.

[7]Lembeck, C. A., and Prussing, J. E., "Optimal Impulsive Intercept with Low-Thrust Rendezvous Return," *Journal of Guidance, Control, and Dynamics*, Vol. 16, No. 3, 1993, pp. 426–433.

[8]Carter, T. E., "New Form for the Optimal Rendezvous Equations near a Keplerian Orbit," *Journal of Guidance, Control, and Dynamics*, Vol. 13, No. 1, 1990, pp. 183–186.

[9]Carter, T., and Brient, J., "Fuel-Optimal Trajectories for Linearized Equations with Application to Keplerian Orbits," *Advances in the Astronautical Sciences*, Vol. 76, Pt. 3, 1992, pp. 2083–2096.

[10]Zarchan, P., *Tactical and Strategic Missile Guidance*, Vol. 176, Progress in Astronautics and Aeronautics, AIAA, Washington, DC, 1997, pp. 263–289.

[11]Nelson, S. L., and Zarchan, P., "Alternative Approach to the Solution of Lambert's Problem," *Journal of Guidance, Control, and Dynamics*, Vol. 15, No. 4, 1992, pp. 1003–1009.

[12]Press, W. H., *Numerical Recipes in FORTRAN: The Art of Scientific Computing*, Cambridge Univ. Press, New York, 1992, p. 406.